Research Article

The Inverse Fundamental Operator Marching Method for Cauchy Problems in Range-Dependent Stratified Waveguides

Peng Li[1,2] and Weizhou Zhong[2]

[1] *Department of Mathematics, North China University of Water Conservancy and Electric Power, Zhengzhou 450011, China*
[2] *School of Economics and Finance, Xi'an Jiaotong University, Xi'an 710061, China*

Correspondence should be addressed to Weizhou Zhong, weizhou@mail.xjtu.edu.cn

The inverse fundamental operator marching method (IFOMM) is suggested to solve Cauchy problems associated with the Helmholtz equation in stratified waveguides. It is observed that the method for large-scale Cauchy problems is computationally efficient, highly accurate, and stable with respect to the noise in the data for the propagating part of a starting field. In further, the application scope of the IFOMM is discussed through providing an error estimation for the method. The estimation indicates that the IFOMM particularly suits to compute wave propagation in long-range and slowly varying stratified waveguides.

1. Introduction

In many engineering applications, efficient mathematical methods are often required for the computing of propagation phenomena and transitions in complex systems. Recently, many interesting works on this issue are proposed to improve efficiencies in many different scientific areas, for example, the wavelet-related method for the integrodifferential and integral equations [1, 2], the exact solution of impulse response to a class of fractional oscillators [3], the representation of a stochastic bound in stochastic modeling [4], the mathematical transform of traveling-wave equations [5] and the dynamics generated by coherent functions [6], the numerical transform for the Helmholtz equation [7]. As one of propagation phenomena and transitions, wave propagation problems associated with the Helmholtz equation are very common and important in many areas, for example, ocean

acoustics, wave propagation and scattering, and electromagnetic field. Many works have been done to improve the computing efficiency in this area.

Some mathematical problems with their boundary conditions not completely known due to some technical difficulties often happen in many scientific and engineering areas described by the Helmholtz equation, such as ocean acoustics, wave propagation and scattering, and electromagnetic field. With the assistance of additionally supplied data, to determine the boundary conditions on the inaccessible part of the boundary or the source condition constitutes the inverse boundary value problem or the Cauchy problem, which is ill posed in the sense that small perturbations in the data may result in an enormous deviation in the solution. Here, the purpose of this study is to improve the efficiency for the computing of the Cauchy problems.

Some numerical methods for medium-scale problems have been proposed for the Cauchy problem [7–22]. However they are not practical for large-scale wave propagation problems, for example, wave propagation in optics and ocean acoustics [23]. Large-scale wave propagation problems in acoustics, electromagnetism, seismic migration, and other applications often require solving the Helmholtz equation in a very large-scale domain with curved interfaces or boundaries. For example, waves are allowed to travel large distances in the horizontal direction in ocean acoustics. For large-scale wave propagation problems, indirect methods, for example, parabolic equation (PE) method [24–26], are widely used, since direct methods like finite element method (FEM) result in very large indefinite linear systems which are hard to be solved. The PE method gives useful approximations to the outgoing component of the wave-field in the case of weak range dependence. However, its accuracy in weakly range-dependent waveguides over large range distances has not been rigorously established [27]. Then, the exact one-way reformulation method [28, 29] which reformulates the Helmholtz equation in terms of the DtN (Dirichlet-to-Neumann) map Q and the fundamental solution operator Y is proposed to solve the wave propagation problem exactly. When the range length scale is much larger than the transverse length scale of the waveguide, such exact reformulation is useful, and numerical methods based on this reformulation feature range-independent memory requirements and linear scaling of computing time.

Based on the exact one-way reformulation, the "inverse fundamental operator marching method" (IFOMM) [23] is developed to reconstruct the propagating parts of incident waves exactly from the received waves in one-layered medium waveguides with curved bottom. While, in many practical applications, the computed waveguides are often multilayered and composed by different mediums with varied densities, and, thus, this study tries to solve the Cauchy problems associated with the Helmholtz equation in multilayered waveguides. Firstly, whether the IFOMM is applicable in multilayered waveguides is the primary question need to be answered. As numerical examples demonstrate, the illnesses caused by the discontinuities between different layers, such as the density and the wavenumber, can also be remedied by the IFOMM successfully and the linear systems arising in the marching process can be treated by the truncated singular value decomposition. Secondly, an error estimation for the numerical marching scheme is provided to discuss the proper scope of the IFOMM's application. The IFOMM is important for inverse problems in many applications in stratified waveguides, for example, source localization and remote sensing in ocean acoustics [30]. For instance, the location of a point source can be determined from the reconstructed propagating part of the incident field.

This paper is arranged as follows. The basic mathematical formulations are described in Section 2. In Section 3, we reorganize the inverse operator marching scheme firstly,

then give the error estimation for the IFOMM and discuss its application scope; interface conditions and matrix approximation are briefly introduced in the end of this section. Section 4 presents some numerical results obtained by IFOMM. We conclude our work with some discussions in Section 5.

2. Mathematical Formulation

Consider the two-dimensional Helmholtz equation in a typical ocean and seabed environment with two curved interfaces

$$u_{xx} + u_{zz} + \kappa^2(x, z)u = 0 \quad -\infty < x < +\infty, \; 0 < z < D_1, \tag{2.1}$$

where the first layer with density ρ_1 is located in $0 < z < h_1(x)$, the second layer with density ρ_2 is located in $h_1(x) < z < h_2(x)$, the third layer with density ρ_3 is located in $h_2(x) < z < D_1$; the interfaces are two curves $z = h_1(x)$ and $z = h_2(x)$, with $D_1 > 1$, $L \gg D_1 \gg 1/k$, u represents the Fourier transform of acoustic pressure, and κ is called wavenumber. We also assume that the problem is range independent (i.e., wavenumber and interfaces are independent of x) for $x \leqslant 0$ and $x \geqslant L$, that is,

$$h_1(x) = \begin{cases} h_{1,0}, & x \leqslant 0, \\ h_{1,\infty}, & x \geqslant L, \end{cases}$$

$$h_2(x) = \begin{cases} h_{2,0}, & x \leqslant 0, \\ h_{2,\infty}, & x \geqslant L, \end{cases} \tag{2.2}$$

$$\kappa(x, z) = \begin{cases} \kappa_0(z), & x \leqslant 0, \\ \kappa_\infty(z), & x \geqslant L. \end{cases}$$

The boundary conditions on the top and the bottom are supposed as $u|_{z=0} = 0$ and $u|_{z=D_1} = 0$. The interface conditions mean that

$$\lim_{z \to h_1(x)^-} u(x, z) = \lim_{z \to h_1(x)^+} u(x, z),$$

$$\frac{1}{\rho_1} \lim_{z \to h_1(x)^-} \frac{\partial u(x, z)}{\partial \mathbf{n}} = \frac{1}{\rho_2} \lim_{z \to h_1(x)^+} \frac{\partial u(x, z)}{\partial \mathbf{n}},$$

$$\lim_{z \to h_2(x)^-} u(x, z) = \lim_{z \to h_2(x)^+} u(x, z), \tag{2.3}$$

$$\frac{1}{\rho_2} \lim_{z \to h_2(x)^-} \frac{\partial u(x, z)}{\partial \mathbf{n}} = \frac{1}{\rho_3} \lim_{z \to h_2(x)^+} \frac{\partial u(x, z)}{\partial \mathbf{n}},$$

where $\mathbf{n}$ is a normal vector of the interface $z = h_1(x)$ or $z = h_2(x)$ (Figure 1). If there is no wave coming from $+\infty$, the exact boundary condition (radiation condition) at $x = L$ is $u_x = i\sqrt{\partial_z^2 + \kappa_\infty^2(z)}u$, where $i = \sqrt{-1}$ and the square root operator is defined in [28].

Figure 1: Sketch map of a waveguide in ocean acoustics.

We will concentrate on solving the equation for $0 \leqslant x \leqslant L$ since the Helmholtz equation can be easily solved by separable variable method for $x \leqslant 0$ or $x \geqslant L$. If there are no waves coming from $+\infty$, the exact boundary condition (radiation condition) at $x = L$ is $u_x = i\sqrt{\partial_z^2 + \kappa_\infty^2(z)}u$, where $i = \sqrt{-1}$ 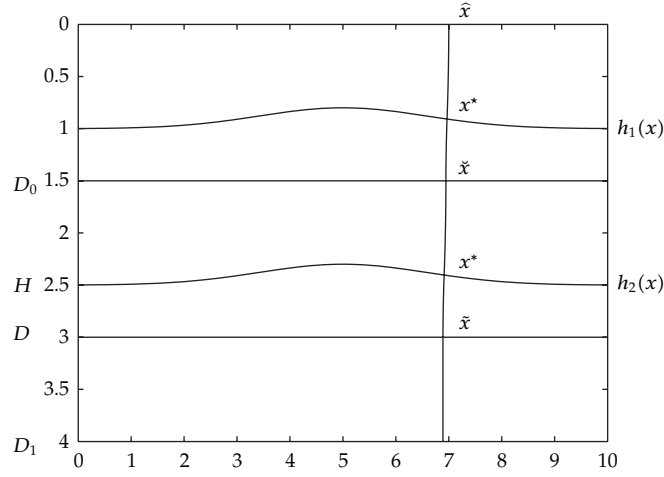and the square root operator is defined in [28]. The simplest boundary condition at $x = 0$ is $u = u_0(z)$ for a given function $u_0(z)$. Here, the dividable assumption is also imposed although it is not necessary [7], there exists one horizontal straight line $z = D_0$ between the interfaces $h_1(x)$ and $h_2(x)$. We suppose that there is an unique solution for (2.1) with the boundary conditions and interface conditions.

The forward problem of (2.1) is to find received wave at $x = L$ from the incident wave at $x = 0$. Whereas, in the inverse boundary value problem or the Cauchy problem presented, the incident wave at $x = 0$ needs to be computed from the received wave at $x = L$. Here, except the radiation condition

$$\frac{\partial u}{\partial x}\Big|_{x=L} = i\sqrt{\partial_z^2 + \kappa_\infty^2(z)}u, \tag{2.4}$$

dirichlet type boundary condition

$$u = u_L(z) \tag{2.5}$$

is imposed. Together with the top, bottom, and interfaces conditions, we seek the solution $u(0, z)$ at $x = 0$ from the imposed boundary conditions at $x = L$.

Since the Helmholtz equation under consideration is in a range-dependent stratified waveguide with some curved interfaces, to flatten the curved interfaces of the dependent waveguide, we perform an analytic local orthogonal transform [31–35] in this study, and the numerical transform [7] is another possible option.

By flattening the stratified waveguide with two curved interfaces through coordinate transformation, (2.6) is expected to be transformed as

$$V_{\hat{x}\hat{x}} + \alpha(\hat{x}, \hat{z})V_{\hat{z}\hat{z}} + \beta(\hat{x}, \hat{z})V_{\hat{z}} + \gamma(\hat{x}, \hat{z})V = 0, \tag{2.6}$$

and details can be referred in [34].

3. Numerical Algorithm

This section reorganizes the operator form of the IFOMM for inverse boundary value problems in multilayered waveguide firstly. An error estimation for the IFOMM is then provided to discuss its properties. In the end, the forward fundamental operator marching method [28, 29, 31–33] (FFOMM) for forward problems is also briefly reviewed for the sake of the comparison with IFOMM.

Let $\{s_j\}$ be a partition of the interval $[0, L]$, that is, $0 = s_0 < s_1 < s_2 < \cdots < s_p = L$, where the solutions are required. Consider also the refined partition $\hat{x} : 0 = \hat{x}_0 < \hat{x}_1 < \hat{x}_2 < \cdots \hat{x}_{s-1} < \hat{x}_s < \hat{x}_{s+1} < \cdots < \hat{x}_m = L$, with $\{s_j\} \subseteq \{\hat{x}_s\}, p \ll m, \ j = 0, 1, 2, \ldots, p, s = 0, 1, 2, \ldots, m.$ Let Q_s and Y_s be the approximations of Q and Y at $\hat{x}_s$, respectively, denote range step size $\tau = \hat{x}_{s+1} - \hat{x}_s$. The forward problem computes the solutions required in $\{s_j\}$ from the incident wave at $\hat{x} = 0$ to $\hat{x} = L$. On the contrary, the Cauchy problem computes the solutions at required places from received wave at $\hat{x} = L$ to the incident wave at $\hat{x} = 0$.

3.1. IFOMM

The DtN operator Q and the fundamental operator Y are defined by

$$V_{\hat{x}} = Q(\hat{x})V, \tag{3.1}$$

$$V(L, \cdot) = Y(\hat{x}; L)V(\hat{x}, \cdot). \tag{3.2}$$

By substituting (3.1) into (2.6) and differentiating (3.2) with respect to $\hat{x}$, the equations for Q and Y are obtained as

$$\frac{dQ}{d\hat{x}} = -Q^2 - \left(\alpha\partial_{\hat{z}}^2 + \beta\partial_{\hat{z}} + \gamma\right), \tag{3.3}$$

$$\frac{dY}{d\hat{x}} = -YQ(\hat{x}). \tag{3.4}$$

The DtN operator Q in range-independent region, that is, $x \geqslant L$, satisfies the analytic "initial" conditions

$$Q(L) = i\sqrt{\alpha(L, \hat{z})\partial_{\hat{z}}^2 + \gamma(L, \hat{z})} \tag{3.5}$$

if there are no waves coming from $+\infty$, and Y satisfies $Y(L, L) = I$.

Equation (2.6) on the interval $(\widehat{x}_{s-1}, \widehat{x}_s)$ is approximated by their midpoint values at $\widehat{x}_{s-1/2} = (\widehat{x}_{s-1} + \widehat{x}_s)/2$. We have the following operator marching scheme in $[s_{j-1}, s_j](s_{j-1} < \widehat{x}_s \leqslant s_j)$

$$B = \sqrt{\alpha(\widehat{x}, \widehat{z})\partial_{\widehat{z}}^2 + \beta(\widehat{x}, \widehat{z})\partial_z + \gamma(\widehat{x}, \widehat{z})}|_{\widehat{x}=\widehat{x}_{s-1/2}},$$

$$P = (Q + iB)^{-1}(-Q + iB),$$

$$R = e^{i\tau B}Pe^{i\tau B}, \tag{3.6}$$

$$Q_{s-1} = iB(I - R)(I + R)^{-1},$$

$$Y_{s-1} = Y_s(I + P)e^{i\tau B}(I + R)^{-1}.$$

For derivation details, we refer to [29, 31]. For simplicity, the shorthand notation

$$\text{OperatorMarching } (Q_s, Y_s; Q_{s-1}, Y_{s-1}) \tag{3.7}$$

is used to represent the operator marching process (3.6).

The inverse fundamental operator marching method can be described as follows.

Algorithm 1 (IFOMM).

Step 1. OperatorMarching $(Q_{s+1}, Y_{s+1}; Q_s, Y_s)$, where $s = m, m - 1, \ldots, 0$.

Step 2. If $\widehat{x}_s = s_i(i = p, \ldots, 1, 2)$, solve $Y_sV_s = V(L, \cdot)$ by TSVD, $i = i - 1$.

Step 3. Let $u(\widehat{x}_s, \cdot) = W(\widehat{x}_s, \cdot)V_s$.

Step 4. If $[\widehat{x}_{s+1}, \widehat{x}_s]=[\widehat{x}_1, \widehat{x}_0]$, end the program, else let $s = s - 1$ and repeat Step 1.

Generally, the *L*-curve method [36] is used to determine the regularization parameter with which the TSVD can work smoothly. In fact, the *L*-curve criterion is not really used in the marching computing since only propagating modes can determine the waves after a long-range propagating, which gives rise to choose the number of propagating modes as the regularization parameter for the TSVD. And it has been verified that the parameter determined by the *L*-curve method is just the number of propagating modes in the waveguide [23].

3.2. Error Estimation

The error estimation for the IFOMM is provided firstly. Based on the estimation, the utilization scope of the method in stratified waveguides is analyzed.

From the operator marching process (3.6), we have

$$\|Y_{s-1}\| \leqslant \|Y_s\| \cdot \|(I + P_s)\| \cdot \left\|e^{i\tau B_s}\right\| \cdot \left\|(I + R_s)^{-1}\right\|, \tag{3.8}$$

where P_s, R_s, B_s, and so forth represent the corresponding operators in interval $[\hat{x}_{s-1}, \hat{x}_s]$, $\|\cdot\| = \|\cdot\|_2$.

Then, recurse the formula (3.8) and notice that $Y_m = I$, $\|I\|_2 = 1$

$$\|Y_{s-1}\| \leqslant \prod_{j=s}^{m} \|(I + P_j)\| \|(I + R_j)^{-1}\| \cdot \prod_{j=s}^{m} \|e^{i\tau B_j}\|. \tag{3.9}$$

In the same way, there is also

$$\|Y_{s-1}^{-1}\| \leqslant \prod_{j=s}^{m} \|(I + P_j)^{-1}\| \|(I + R_j)\| \cdot \prod_{j=s}^{m} \|e^{-i\tau B_j}\|. \tag{3.10}$$

According to (3.2), there are

$$Y_{s-1} \cdot V_{s-1} = V_m, \tag{3.11}$$

$$V_{s-1} = Y_{s-1}^{-1} \cdot V_m. \tag{3.12}$$

By taking norm to (3.12) and utilizing(3.10)

$$\|V_{s-1}\| \leqslant \|Y_{s-1}^{-1}\| \cdot \|V_m\| = \prod_{j=s}^{m} \|(I + P_j)^{-1}\| \|(I + R_s)\| \cdot \prod_{j=s}^{m} \|e^{-i\tau B_j}\| \cdot \|V_m\|. \tag{3.13}$$

Suppose that $\tilde{V}_m$ be polluted and $\tilde{V}_{s-1}$ be obtained by (3.12), we have

$$V_{s-1} - \tilde{V}_{s-1} = Y_{s-1}^{-1} \cdot \left(V_m - \tilde{V}_m\right) \tag{3.14}$$

from (3.12) and

$$\|V_{s-1} - \tilde{V}_{s-1}\| \leqslant \prod_{j=s}^{m} \|(I + P_j)^{-1}\| \|(I + R_j)\| \cdot \prod_{j=s}^{m} \|e^{-i\tau B_j}\| \cdot \|V_m - \tilde{V}_m\| \tag{3.15}$$

according to (3.10). If $e_{s-1} = V_{s-1} - \tilde{V}_{s-1}$, $e_m = V_m - \tilde{V}_m$, we have the following theorem.

Theorem 3.1. *Let $e_m = V_m - \tilde{V}_m$ be the initial measurement error, then, the resulting errors of the IFOMM solution V_{s-1} at $\hat{x} = s_{j-1}$, $e_{s-1} = V_{s-1} - \tilde{V}_{s-1}$ will satisfy*

$$\|e_{s-1}\| \leqslant \prod_{j=s}^{m} \|(I + P_j)^{-1}\| \|(I + R_j)\| \cdot \prod_{j=s}^{m} \|e^{-i\tau B_j}\| \cdot \|\varepsilon_m\|. \tag{3.16}$$

Corollary 3.2. *For weakly range-dependent stratified waveguides, if there exist a constant C, subject to $\prod_{j=s}^{m} \|(I + P_j)^{-1}\| \|(I + R_j)\| \leqslant C$, with $s = 1, 2, \ldots, m$, the IFOMM is stable.*

Proof. In weakly range-dependent waveguides, the reflection waves are very weak which leads to $\|P_s\| \approx 0$ and $\|R_s\| \approx 0$. For a grid which approximates the computed domain and the PDE model enough accurately, there exists a positive constant $C = \max_{s=1,2,\ldots,m} \prod_{j=s}^{m} \|(I + P_j)^{-1}\| \|(I + R_j)\|$ satisfies that $\prod_{j=s}^{m} \|(I + P_j)^{-1}\| \|(I + R_j)\| \leqslant C$, with $s = 1, 2, \ldots, m$. For an $m + 1$ points discretization along range direction, we have

$$\|e_{s-1}\| \leqslant C \prod_{j=s}^{m} \|e^{-i\tau B_j}\| \cdot \|e_m\| \tag{3.17}$$

from (3.16).

The operators $B_j (j = m, m - 1, \ldots, 1)$ are truncated by the number of propagating modes, the eigenvalues left for the truncated system are positive real which gives rise to $\|e^{-i\tau B_j}\|_2 = 1$. Thus,

$$\|e_{s-1}\| \leqslant C \|e_m\|. \tag{3.18}$$

When the reflections for every mode are weak in the waveguide, the constant C will be small for a enough slim grid. Thus, the IFOMM is stable.   □

A more slim grid may approximate the original problem certainly, while in the same time, it may also amplify the initial errors if the number of discrete points in range direction tend to the infinite. Since large-range step method is used to discretize the computed domain for slowly varied waveguides and overdense grid is of no need for obtaining required accuracy, the IFOMM is stable in weakly range-dependent waveguides without much reflections according to the corollary.

The theorem gives two major factors which affect the IFOMM solutions of (2.6) greatly. One is to choose correct number for truncating the linear systems, the other is that the reflection in the waveguide can not be very strong. Strong reflection may lead to a very large $C = \max_{s=1,2,\ldots,m} \prod_{j=s}^{m} \|(I + P_j)^{-1}\| \|(I + R_j)\|$ in (3.18), since every $\|(I + P_j)^{-1}\|$ can be very large.

3.3. Interface Conditions and Matrix Approximation

The formulas in (3.6) have to be further discretized with matrices replacing the operators [29, 32]. The interface and boundary conditions are important in the discretization. Corresponding to the interface and boundary conditions of (2.1), we need to consider the interface and boundary conditions for the improved Helmholtz equation (2.6). Details can be referred in [34].

Furthermore, we approximate the operator

$$B(\widehat{x}, \widehat{z}) = \alpha(\widehat{x}, \widehat{z})\partial_{\widehat{z}}^2 + \beta(\widehat{x}, \widehat{z})\partial_{\widehat{z}} + \gamma(\widehat{x}, \widehat{z}) \tag{3.19}$$

by an $N \times N$ tridiagonal matrix $A(\widehat{x})$. Details can be referred in [32].

3.4. FFOMM

Let the DtN operator Q and the fundamental operator Y satisfy

$$V_{\hat{x}} = Q(\hat{x})V, \qquad V(\hat{x}', \cdot) = Y(\hat{x}; \hat{x}')V(\hat{x}, \cdot). \tag{3.20}$$

By substituting (3.20) into (2.6), formulas for Q and Y can be derived analogously. Using the operator marching scheme (3.6) for the FFOMM from $\hat{x} = L$ to $\hat{x} = 0$, its fundamental operator $Y(s_j; s_{j+1})$ can be determined. For more details, we refer to [28]. The FFOMM can be written as the following algorithm.

Algorithm 2 (FFOMM).

Step 1. OperatorMarching$(Q_{s+1}, Y_{s+1}; Q_s, Y_s)$, where $s = m, m-1, \ldots, 0$.

Step 2. If $\hat{x}_s = s_i (i = p, \ldots 2, 1)$ Save $Y_s, i = i - 1$ and reset $Y_s = I$.

Step 3. If $[\hat{x}_{s+1}, \hat{x}_s] \neq [\hat{x}_1, \hat{x}_0]$, $s = s - 1$ repeat Step 1, else go to Step 4.

Step 4. Load Y_{s_i}, $V(s_i, \cdot) = Y_{s_i} V_{s_{i-1}}$.

Step 5. Load $u(\hat{x}_s, \cdot) = W(\hat{x}_s, \cdot)V_s$.

Step 6. If $[\hat{x}_{s+1}, \hat{x}_s] = [\hat{x}_m, L]$, end the program, else let $s = s + 1$ repeat Step 1.

If similar error analysis of the IFOMM is applied to the FFOMM, similar result can be obtained. The conditions on which the Helmholtz equation can be exactly solved by the FFOMM also demand that the reflection of the propagating modes be small in the waveguide.

4. Numerical Example

A typical numerical example in ocean acoustics is provided here to examine the IFOMM for solving Cauchy problems in stratified waveguides.

Example 4.1. Let

$$\kappa = \begin{cases} 16, & 0 < z < h_1(x), \\ 0.7 \times 16, & h_1(x) < z < h_2(x), \\ 0.2 \times 16, & h_2(x) < z < D_1, \end{cases} \tag{4.1}$$

with $L = 10$, $n = 30$, $D_0 = 1.5$, $H = 2.5$, $D = 3$, $D_1 = 4$, $N = 400$, $\rho_1 = 1$, $\rho_2 = 1.7$, $\rho_3 = 2.7$, $\delta = 0.025$, $h_1(x) = 1 - \varepsilon_1 e^{-\sigma_1((x/L)-(1/2))^2}$, $h_2(x) = H - \varepsilon_2 e^{-\sigma_2((x/L)-(1/2))^2}$, $\varepsilon_1 = \varepsilon_2 = 0.1$, $\sigma_1 = \sigma_2 = 10$, $0 \leqslant z \leqslant 4$, $0 \leqslant x \leqslant 10$, where N is the number of points to discretize the $\hat{z}$ variable, n is the number to truncate the $N \times N$ matrices that approximate the operators arising in the marching process [32].
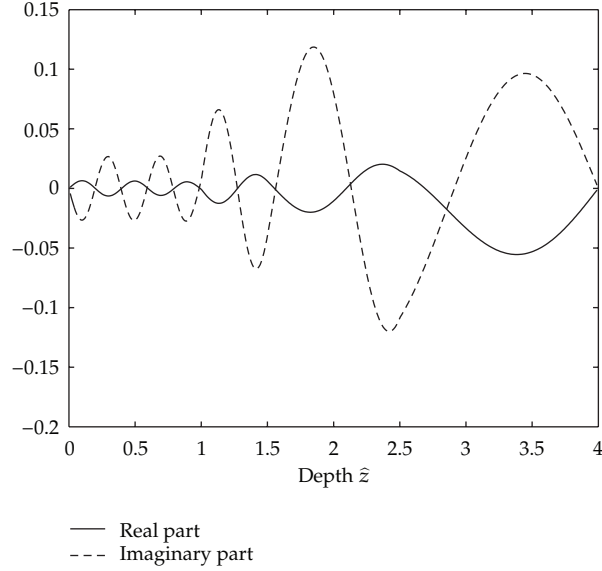
Figure 2: The received wave $u(L, \hat{z})$ of Case 1.

Suppose incident wave u_0 at $\hat{x} = 0$ is $V_{N-9}^{(L)}$ (Case 1: the tenth propagation mode at $\hat{x} = L$) and $V_N^{(L)}$ (Case 2: the first propagation mode at $\hat{x} = L$), respectively, reconstruct the incident wave.

The numerical example takes the incident wave at $\hat{x} = 0$ as the reference solution for the IFOMM solution. Although varied range step size considering the character of the range-dependent waveguide is more reasonable, we will choose constant range step size for simplicity. The solutions are computed with a large range step size $\tau = 1/8$ ($m = 80$). As the numerical test shows, the reasonably accurate reformulated solutions are already obtained for $\tau = 1/8$.

In practice, the available data is usually contaminated by measurement errors, and the stability of the numerical method is of vital importance for obtaining physically meaningful results. To this end, the simulated noisy data generated by

$$\tilde{u}_m = [v_1, v_2, \ldots, v_{n_0}] \operatorname{Re}(\chi_m)(1 + \varepsilon \zeta_1) + i \operatorname{Im}(\chi_m)(1 + \varepsilon \zeta_2), \quad j = 1, 2, \ldots, N, \qquad (4.2)$$

is used to impose on the received wave $u_m = u(\hat{x}_m, \hat{z})$, where $[v_1, v_2, \ldots, v_{n_0}]$ is the eigenvectors corresponding to the propagating modes of the operator (3.19) at $\hat{x} = L$ and n_0 is the number of propagating modes, $u_m = [v_1, v_2, \ldots, v_{n_0}] \cdot \chi_m$, χ_m is an n_0-dimensional vector, ζ_1 and ζ_2 are normally distributed random variables with zero mean and unit standard deviation, respectively, and ε dictates the level of data noise which represents the ratio of noise energy to data energy in 2-norm. The random variable ζ_1 and ζ_2 are realized by using the Fortran function of IMSL library DRNNOF().

Figures 2 and 5 denote the received waves $u(L, \hat{z})$ of Case 1 and 2, respectively. Figures 3 and 6 give the reconstructed incident waves $u(0, \hat{z})$ which are computed by the IFOMM with TSVD where regularization parameter is chosen as 10 (the number of the propagation modes in the waveguide). As indicated by Figures 3 and 6, the regularization solution $u(0, \hat{z})$
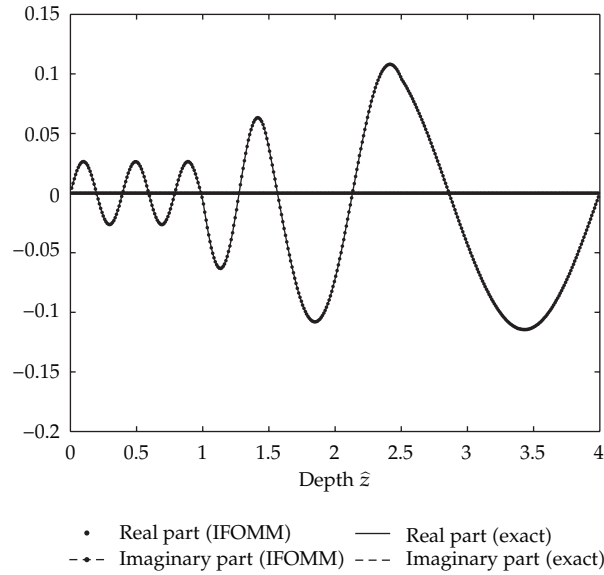
Figure 3: Comparison with $u(0, \hat{z})$ of Case 1 for the exact incident wave and the solution obtained by IFOMM.
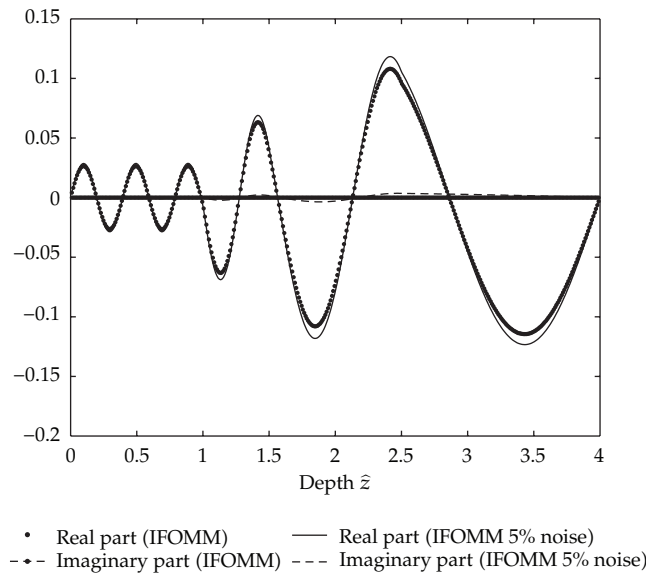

Figure 4: Comparison with $u(0, \hat{z})$ of Case 1 for the solution obtained by IFOMM with no noise and 5% noise.

computed by the IFOMM is in good agreement with the exact incident wave u_0. As shown by the solutions obtained with noise level $\varepsilon = 5\%$ in Figures 4 and 7, the reconstruction remains very stable despite the high noise level. The performance of the IFOMM for the two different incident waves of Cases 1 and 2 verifies that the proposed algorithm is efficient, accurate, and stable for the incident waves.
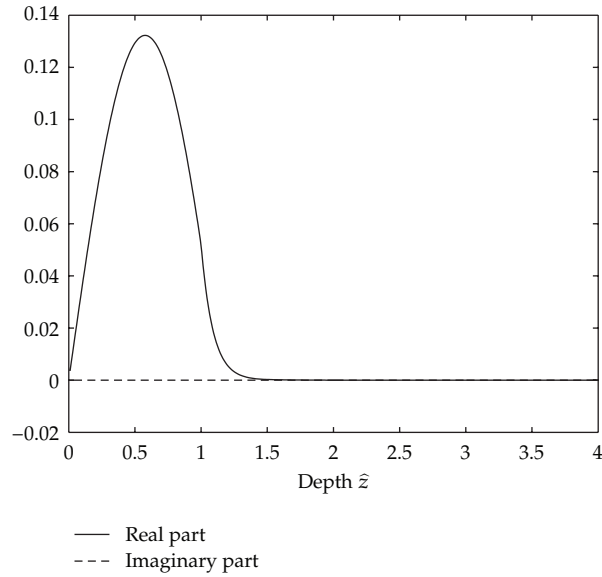
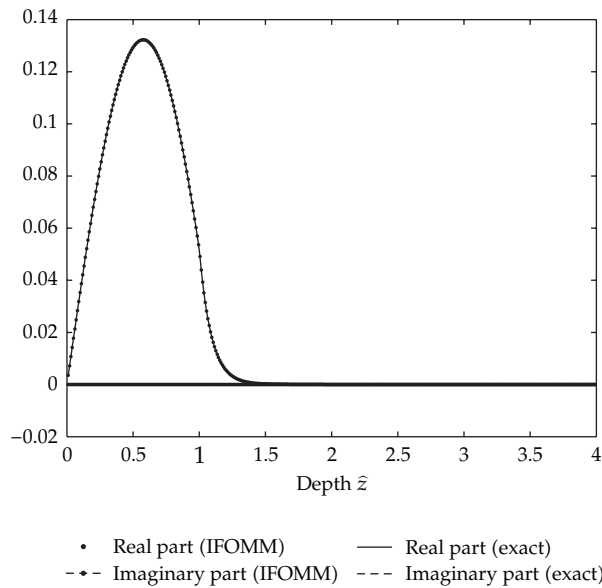**Figure 5:** The received wave $u(L, \hat{z})$ of Case 2.

Figure 6: Comparison with $u(0, \hat{z})$ of Case 2 for the exact incident wave and the solution obtained by IFOMM.

5. Conclusion

The IFOMM developed in one-layered waveguides is applied to solve inverse boundary value problems associated with the Helmholtz equation in stratified waveguides. Numerical example demonstrates that the IFOMM can be used to compute inverse boundary problems in the stratified waveguides successfully. The scope of the IFOMM's application is then
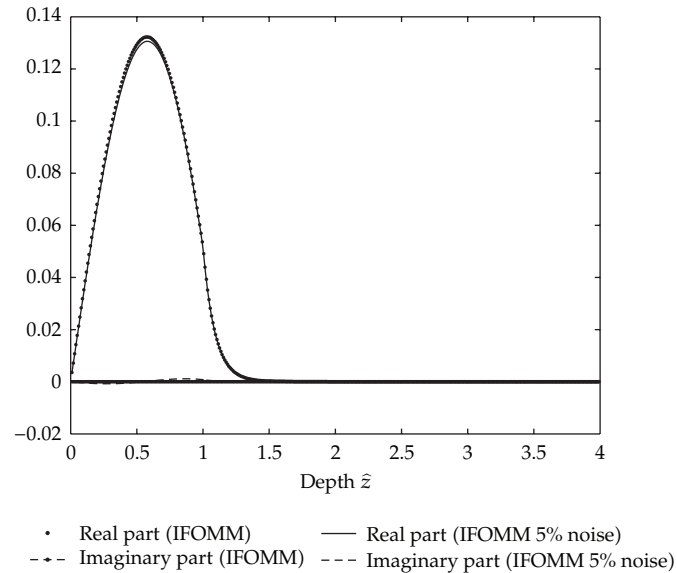
Figure 7: Comparison with $u(0, \hat{z})$ of Case 2 for the solution obtained by IFOMM with no noise and 5% noise.

discussed based on an error estimation for the marching scheme. The estimation gives a quantitative estimate of error propagation and shows that IFOMM can only be applied in waveguides where reflection is not strong. In further, the theorem also reveals that the errors may be cumulated greatly in some special circumstances when the grid becomes excessive fine. Numerical examples indicate that the IFOMM is computationally efficient, highly accurate, and stable with respect to the noise in the data for the propagating part of a starting field when the computing domain is long and complex.

There are several further studies related to the IFOMM for solving the Cauchy problems. Firstly, although the IFOMM only considers two-dimensional problems in its current form, the scheme is easily extended to problems in three-dimensional space under cylindrical coordinates, and it can also be extended to solve wave propagation under three-dimensional Cartesian coordinate system. Secondly, when the number of propagating modes varies with the range direction frequently, which is corresponding to some of propagating modes that are totally reflected, whether the IFOMM or FFOMM can be applied through some improvements of them in such waveguides, and how to improve the methods? At least, the parameters for truncating the systems are a little more difficult to be determined. Thirdly, the estimation for error propagation may be improved through more detailed analysis.

Acknowledgment

References

[1] C. Cattani, "Shannon wavelets for the solution of integrodifferential equations," *Mathematical Problems in Engineering*, vol. 2010, Article ID 408418, 22 pages, 2010.

[2] C. Cattani and A. Kudreyko, "Harmonic wavelet method towards solution of the Fredholm type integral equations of the second kind," *Applied Mathematics and Computation*, vol. 215, no. 12, pp. 4164–4171, 2010.

[3] M. Li, S. C. Lim, and S. Y. Chen, "Exact solution of impulse response to a class of fractional oscillators and its stability," *Mathematical Problems in Engineering*, vol. 2011, Article ID 657839, 9 pages, 2011.

[4] M. Li and W. Zhao, "Representation of a stochastic traffic bound," *IEEE Transactions on Parallel and Distributed Systems*, vol. 21, no. 9, pp. 1368–1372, 2010.

[5] E. G. Bakhoum and C. Toma, "Mathematical transform of traveling-wave equations and phase aspects of quantum interaction," *Mathematical Problems in Engineering*, vol. 2010, Article ID 695208, 15 pages, 2010.

[6] E. G. Bakhoum and C. Toma, "Specific mathematical aspects of dynamics generated by coherence functions," *Mathematical Problems in Engineering*, vol. 2011, 10 pages, 2011.

[7] P. Li, W. Z. Zhong, G. S. Li, and Z. H. Chen, "A numerical local orthogonal transform method for stratified waveguides," *Journal of Zhejiang University*, vol. 11, no. 12, pp. 998–1008, 2010.

[8] M. R. Bai, "Application of BEM (boundary element method)-based acoustic holography to radiation analysis of sound sources with arbitrarily shaped geometries," *Journal of the Acoustical Society of America*, vol. 92, pp. 533–549, 1992.

[9] Z. Wang and S. F. Wu, "Helmholtz equation least-squares method for reconstructing the acoustic pressure field," *Journal of the Acoustical Society of America*, vol. 102, no. 4, pp. 2020–2032, 1997.

[10] S. F. Wu and J. Yu, "Reconstructing interior acoustic pressure fields via Helmholtz equation least-squares method," *Journal of the Acoustical Society of America*, vol. 104, no. 4, pp. 2054–2060, 1998.

[11] T. Delillo, V. Isakov, N. Valdivia, and L. Wang, "The detection of the source of acoustical noise in two dimensions," *SIAM Journal on Applied Mathematics*, vol. 61, no. 6, pp. 2104–2121, 2001.

[12] T. DeLillo, V. Isakov, N. Valdivia, and L. Wang, "The detection of surface vibrations from interior acoustical pressure," *Inverse Problems*, vol. 19, no. 3, pp. 507–524, 2003.

[13] L. Marin, L. Elliott, P. J. Heggs, D. B. Ingham, D. Lesnic, and X. Wen, "Conjugate gradient-boundary element solution to the Cauchy problem for Helmholtz-type equations," *Computational Mechanics*, vol. 31, no. 3, pp. 367–372, 2003.

[14] L. Marin, L. Elliott, P. J. Heggs, D. B. Ingham, D. Lesnic, and X. Wen, "An alternating iterative algorithm for the Cauchy problem associated to the Helmholtz equation," *Computer Methods in Applied Mechanics and Engineering*, vol. 192, no. 5-6, pp. 709–722, 2003.

[15] L. Marin, L. Elliott, P. J. Heggs, D. B. Ingham, D. Lesnic, and X. Wen, "Comparison of regularization methods for solving the Cauchy problem associated with the Helmholtz equation," *International Journal for Numerical Methods in Engineering*, vol. 60, no. 11, pp. 1933–1947, 2004.

[16] L. Marin, L. Elliott, P. J. Heggs, D. B. Ingham, D. Lesnic, and X. Wen, "BEM solution for the Cauchy problem associated with Helmholtz-type equations by the Landweber method," *Engineering Analysis with Boundary Elements*, vol. 28, no. 9, pp. 1025–1034, 2004.

[17] B. T. Jin and Y. Zheng, "A meshless method for some inverse problems associated with the Helmholtz equation," *Computer Methods in Applied Mechanics and Engineering*, vol. 195, no. 19–22, pp. 2270–2288, 2006.

[18] B. T. Jin and Y. Zheng, "Boundary knot method for some inverse problems associated with the Helmholtz equation," *International Journal for Numerical Methods in Engineering*, vol. 62, no. 12, pp. 1636–1651, 2005.

[19] B. T. Jin and Y. Zheng, "Boundary knot method for the Cauchy problem associated with the inhomogeneous Helmholtz equation," *Engineering Analysis with Boundary Elements*, vol. 29, no. 10, pp. 925–935, 2005.

[20] L. Marin and D. Lesnic, "The method of fundamental solutions for the Cauchy problem associated with 2D Helmholtz-type equations," *Computers & Structures*, vol. 83, no. 4-5, pp. 267–278, 2005.

[21] L. Marin, "A meshless method for the numerical solution of the Cauchy problem associated with 3D Helmholtz-type equations," *Applied Mathematics and Computation*, vol. 165, no. 2, pp. 355–374, 2005.

[22] B. T. Jin and L. Marin, "The plane wave method for inverse problems associated with Helmholtz-type equations," *Engineering Analysis with Boundary Elements*, vol. 32, no. 3, pp. 223–240, 2008.

[23] P. Li, Z. H. Chen, and J. X. Zhu, "An operator marching method for inverse problems in range-dependent waveguides," *Computer Methods in Applied Mechanics and Engineering*, vol. 197, no. 49-50, pp. C4077–C4091, 2008.

[24] F. B. Jensen, W. A. Kuperman, M. B. Porter, and H. Schmidt, *Computational Ocean Acoustics*, American Institute of Physics, New York, NY, USA, 1994.

[25] L. Fishman, "One-way wave propagation methods in direct and inverse scalar wave propagation modeling," *Radio Science*, vol. 28, no. 5, pp. 865–876, 1993.

[26] L. Fishman, A. K. Gautesen, and Z. Sun, "Uniform high-frequency approximations of the square root Helmholtz operator symbol," *Wave Motion*, vol. 26, no. 2, pp. 127–161, 1997.

[27] J. X. Zhu and Y. Y. Lu, "Validity of one-way models in the weak range dependence limit," *Journal of Computational Physics*, vol. 12, no. 1, pp. 55–66, 2004.

[28] Y. Y. Lu and J. R. McLaughlin, "The Riccati method for the Helmholtz equation," *Journal of the Acoustical Society of America*, vol. 100, no. 3, pp. 1432–1446, 1996.

[29] Y. Y. Lu, "One-way large range step methods for Helmholtz waveguides," *Journal of Computational Physics*, vol. 152, no. 1, pp. 231–250, 1999.

[30] M. D. Collins and W. A. Kuperman, "Inverse problems in ocean acoustics," *Inverse Problems*, vol. 10, no. 5, pp. 1023–1040, 1994.

[31] Y. Y. Lu, J. Huang, and J. R. McLaughlin, "Local orthogonal transformation and one-way methods for acoustic waveguides," *Wave Motion*, vol. 34, no. 2, pp. 193–207, 2001.

[32] J. X. Zhu and Y. Y. Lu, "Large range step method for acoustic waveguide with two layer media," *Progress in Natural Science*, vol. 12, no. 11, pp. 820–825, 2002.

[33] Y. Y. Lu and J. X. Zhu, "A local orthogonal transform for acoustic waveguides with an interval interface," *Journal of Computational Physics*, vol. 12, no. 1, pp. 37–53, 2004.

[34] J. X. Zhu and P. Li, "Local orthogonal transform for a class of acoustic waveguides," *Progress in Natural Science*, vol. 17, no. 10, pp. 18–28, 2007.

[35] J. X. Zhu and P. Li, "The mathematical treatment of wave propagation in the acoustical waveguides with n curved interfaces," *Journals of Zhejiang University*, vol. 9, no. 10, pp. 1463–1472, 2008.

[36] P. C. Hansen, "Analysis of discrete ill-posed problems by means of the L-curve," *SIAM Review*, vol. 34, no. 4, pp. 561–580, 1992.